PROCEEDINGS OF SCIENCE

Time, position and orientation calibration using atmospheric muons in KM3NeT

Louis Bailly-Salins[a,*] **on behalf of the KM3NeT collaboration**

[a] *Université de Caen Normandie, ENSICAEN, CNRS/IN2P3, LPC Caen UMR 6534, F-14000 Caen, France*

E-mail: baillysalins@lpccaen.in2p3.fr

The KM3NeT collaboration operates two Cherenkov neutrino telescopes in the deep Mediterranean sea, ORCA and ARCA. Both detectors consist of an array of light-sensitive detectors called Digital Optical Modules (DOMs) assembled along vertical strings anchored to the seafloor. Although the abundant muon flux from cosmic ray air showers is a background for the main scientific objectives of KM3NeT/ORCA and KM3NeT/ARCA, it can be exploited in various ways for calibration purposes. In this contribution, the methods implemented within the KM3NeT calibration workflow which exploit the muon track reconstruction are presented. For the latter, a likelihood fit of a track hypothesis to a set of observed hits on the DOMs is performed. For calibration purposes, the optimal position, time reference and orientation of each string of the detector can be found as the parameters maximizing the overall likelihood of reconstructed muon tracks. The muon track quality method is shown to reach the desired accuracy in time and position, allowing for the determination of the relative time offsets between strings. It also represents an important tool to cross-check position and orientation calibrations obtained by other means. Another muon-based calibration method is used to determine the relative time offsets between DOMs. It is based on the evaluation of the difference between the measured hit time and the one predicted from the fitted muon track's position.

38th International Cosmic Ray Conference (ICRC2023)
26 July - 3 August, 2023
Nagoya, Japan

*Speaker

PoS(ICRC2023)218

1. Introduction

The KM3NeT collaboration [1] operates two Cherenkov neutrino telescopes in the deep Mediterranean sea. ORCA (*Oscillation Research with Cosmics in the Abyss*) is designed to measure atmospheric neutrinos oscillations, while ARCA (*Astroparticle Research with Cosmics in the Abyss*) is designed to detect neutrinos from astrophysical sources. ARCA and ORCA share the same technology and detector elements. Both detectors are instrumented with photomultiplier tubes (PMTs) for the detection of the Cherenkov light emitted by the relativistic charged particles produced in neutrino interactions. KM3NeT detectors consist in a 3-D array of glass-spheres named Digital Optical Modules (DOMs) housing 31 3-inch PMTs each. The DOMs are arranged along vertical strings called Detection Units (DU). Each DU hosts 18 DOMs, is anchored to the seabed and remains vertical due to the buoyancy of the DOMs and to a buoy tied on its top. When completed, each detector "building block" will consist of 115 DUs arranged side by side following a cylindrical footprint. The geometry of ARCA is optimised to maximise its detection efficiency in the energy range 1 TeV-10 PeV, while ORCA is built to detect neutrinos in the range 1-100 GeV. This translates into a different spacing between the DOMs: the vertical and horizontal distances between the DOMs of ORCA are respectively 9 meters and 20 meters, while for ARCA, the corresponding distances are 36 and 90 meters.

To be able to reconstruct accurately the direction of neutrino events, the PMTs need to be synchronized with a 1 ns precision, and their position determined with an accuracy of 20 cm. The orientation of the optical modules must also be known with a precision of 3°. To calibrate the detector in time, position and orientation, several procedures using data from dedicated instruments located inside the DOMs [2], on DU bases or on the seafloor, as well optical data from the PMTs, are used.

2. Calibration of KM3NeT detectors

2.1 Position and orientation calibration

The KM3NeT positioning system [3] relies on a set of acoustic emitters and receivers. The emitters are beacons anchored on the seabed near the detector. There are two sets of acoustic receivers: hydrophones located on the DU bases, and piezoelectric sensors glued at the South pole of the DOMs. The position of each DOM is determined using triangulation of the acoustic signals, constrained by a mechanical model for the DUs. For the orientation calibration, an attitude and heading reference system (AHRS), referred to as "compass", is used. It consists of a set of accelerometers and magnetometers mounted on the electronics boards of each DOM. An important specificity of KM3NeT detectors is that the DOMs move and rotate over time due to sea currents. Thus, dynamic position and orientation calibration procedures have been developped [4], updating the positions and orientations of the DOMs every 10 minutes. The expected accuracies of those dynamic position and orientation calibrations are less than 10 cm and a few degrees, respectively.

2.2 Time calibration

Because of delays arising at different levels of the infrastructure, the time calibration of KM3NeT detectors must be achieved at various scales [5] to synchronize all PMTs:

- inter-PMT (or intra-DOM): synchronize the individual photomultiplier tubes inside a given DOM. This is done using the light resulting from the β^- decay of Potassium-40 naturally present in sea water, which can be detected as coincident hits on a few neighboring PMTs.
- inter-DOM: synchronize the optical modules of a given detection unit. A preliminary calibration is done before deployment of the DU in the sea, using a laser source. In-situ, light pulse emitters located on the DOMs, called nanobeacons and developped by the collaboration [6], are used to adjust the inter-DOM time calibration[7]. Atmospheric muons can also be used for cross-checks (see Section 3.4).
- inter-DU: synchronize the detection units forming the building block. There is currently no dedicated instrument for this inter-DU time calibration. Instead, the muon track quality method, using the reconstructed tracks of the detected atmospheric muons, has been developped. This method will be described in the following sections of the current contribution.

3. Calibration with reconstructed atmospheric muon tracks

3.1 Atmospheric muons in KM3NeT

Cosmic rays are charged particles arriving on the Earth atmosphere with very high kinetic energy. They interact with air nuclei in the upper atmosphere and produce showers. Among the charged secondary particles produced, muons are the most penetrating. The atmospheric muons with enough energy can reach KM3NeT/ORCA and KM3NeT/ARCA [8]. Although forming a background for the main physics goals of KM3NeT, atmospheric muons can be used for cosmic ray physics, as well as for checking the detector performance [9] and for calibration.

3.2 Muon track reconstruction

During data acquisition, a *hit* is produced when a photon reaching a PMT induces an electrical signal above a defined threshold. The hit information includes a time stamp, a time-over-threshold (not relevent in the following), and the geometrical properties of the PMT detecting the hit: position and orientation. A series of causally-connected hits forms an *event*. Muon track reconstruction algorithms process an event by fitting its observed hits with the hypothesis of a straight track of a muon emitting Cherenkov light at a fixed angle along its trajectory. Fitting a muon track to observed hits on PMTs in a non-linear problem. In KM3NeT, an approach with several consecutive steps is employed. The principal step of the fit, determining the direction and vertex position of the track, adopts a maximum likelihood approach. The likelihood is a quantity which describes the agreement between the track hypothesis and the properties of the observed hits. In other words, it describes the *quality* of the track hypothesis. The *best track* is the one maximizing the likelihood.

3.3 Track quality method

The principle of the track quality method (TQM) [10] is to add, on top of the track reconstruction process during which the best track properties are found, a step where the best hit properties are found. Indeed, the likelihood of a reconstructed track depends both on the track properties and on the observed hit properties. As the hit properties are the properties of the PMTs being hit

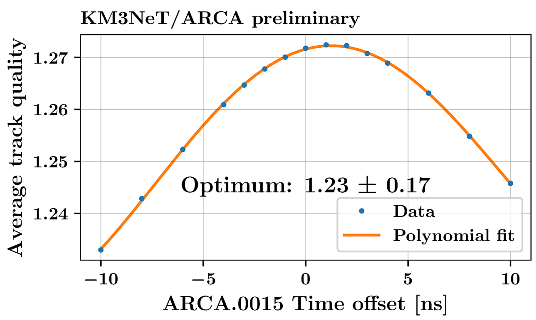

Figure 1: Track quality scan for the time offset of the DU 15 of ARCA. The metric for track quality is the likelihood resulting from the fit of the track divided by the number of hits used in the fit.

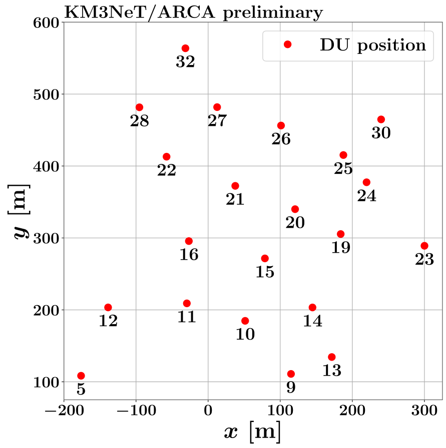

Figure 2: Footprint of the ARCA detector in its 21-DU configuration.

(reference time, position and orientation), finding the best hit properties is equivalent to calibrating the detector. Thus, the optimal calibration can be determined by reconstructing the same data with different values of some detector parameters and monitoring the quality of the reconstructed tracks.

The current implementation of the TQM works at the Detection Unit scale. One-dimensional track quality scans are performed over some parameters of an individual DU (keeping the parameters of other DUs fixed): the time reference of the DU; its position along the x,y, and z axis; and its orientation around the z-axis. An example is shown on Figure 1 for the time calibration of a DU of ARCA. The time offset is relative to a given nominal time calibration. It is applied to all the DOMs of the DU considered. Here, the optimal offset obtained with the muon track quality method is around 1.2 ns, meaning that the reference time of that DU should be shifted by 1.2 ns. The TQM is currently the standard way to obtain the time calibration at the inter-DU scale. For position and orientation calibrations, the TQM is an important tool to cross-check results from the nominal calibration obtained with acoustic data and compasses (see Section 2.1).

It should be highlighted that the TQM is only a relative calibration method. The quality of reconstructed tracks will only be affected by relative shifts in the time, position and orientation of an individual DU with respect to the rest of the detector. For instance, if all the DUs are shifted by 1 m in a given direction, then the reconstructed position of the track will be shifted by 1 m, but its quality will not change. In addition, the accuracy of the method will be worse for DUs which are more isolated from the others, like DU 5, 23 or 32 of ARCA (see Figure 2).

3.4 Hit time residuals method

Another calibration method using reconstructed muon tracks relies on the hit time residuals. Once a muon track is reconstructed, the expected arrival time of a photon on each PMT can be computed under the hypothesis of non-scattered Cherenkov photon. The expected hit time can then be compared with the observed hit time: the difference is called the *hit time residual* (HTR). This method can be used to measure the inter-DOM time offset by fitting the distribution of HTR for each DOM: the difference in HTR value between DOMs is the inter-DOM offset to correct for.

4. Results of the muon track quality method

4.1 Position calibration

The track quality method is important to check the results from the position calibration resulting from acoustic data. In particular, it highlights the improvement in positionning coming from the use of a dynamic calibration, where the position of the DOMs is updated every 10 minutes, rather than a static calibration where the fit of acoustic data is done only once and the movement of the DOMs is neglected. To make that comparison, the same track quality scan as the one shown in Figure 1 can be done on consecutive sets of events. That way, the evolution over time of the optimal offset found with the muon track quality, with respect to the nominal calibration relying on acoustics, can be monitored. An example is shown in Figure 3 for one string of ARCA, covering a period of 86 h where the sea currents were among the highest ever observed on the site. With the static calibration, an evolving x-position offset of several meters is seen with the TQM with respect to the acoustic positioning: this means that due to sea currents, the DU is moving relative to other DUs. This displacement is not accounted for by static calibration. Using dynamic positioning, the offset found with the TQM is very close to zero and almost constant over time, showing that dynamic calibration indeed corrects for the displacement of the strings.

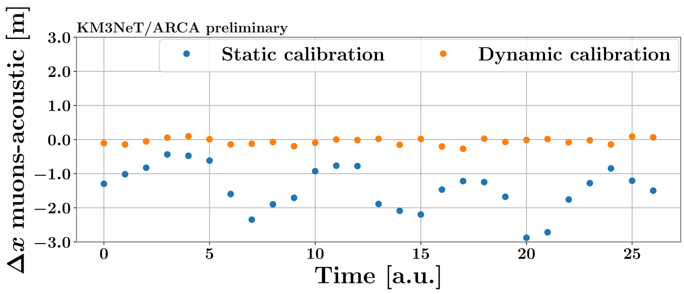

Figure 3: Evolution of the optimal x-position offset with respect to the acoustic positionning obtained with the track quality method, for the DU 15 of ARCA, over a period of 86 h. Each point corresponds to the optimal offset on a set of 5000 consecutive events.

The distribution of the optimal offsets obtained with the TQM for the 21 currently deployed DUs of ARCA is shown in Figure 4. These are obtained for the same period as in Figure 3, both with a static and dynamic position calibration. The same effect is seen for all DUs: when using dynamic calibration, the offsets seen from the muon tracks are much lower, and the spread of that offset over time drastically reduces. This shows that the movement of the DOMs is correctly accounted for.

For ORCA, the relative displacements of each DU with respect to the rest of the detector are much smaller, even in periods of high sea currents, because the DUs are much closer to one another (20 meters appart) than in ARCA (90 meters apart), so they move in currents of similar strength and direction. This is illustrated in Figure 5, where the y-position offset obtained with the TQM with respect to the acoustic position calibration is already very small (around 10 cm on average) with a small spreading of values. As 10 centimeters is essentially the accuracy of the track quality method for ORCA [10], using dynamic calibration does not bring a substantial improvement.

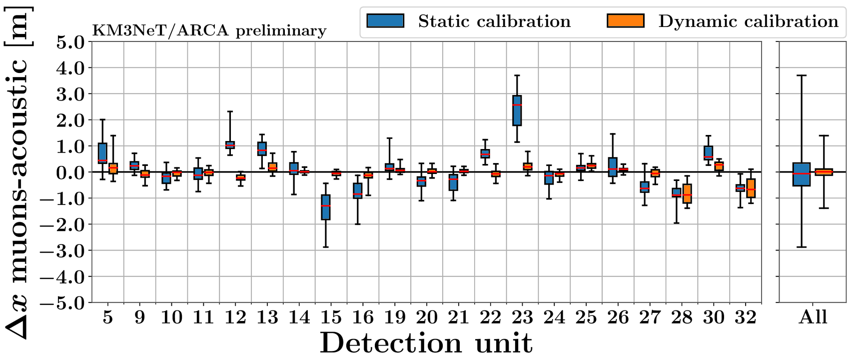

Figure 4: Distribution of the optimal x-position offset obtained with the track quality method with respect to the position calibration from acoustics, shown for each individual DU of ARCA and for all DUs. One entry is an optimal offset on a set of 5000 consecutive events. The boxes contain 50% of the DU entries (between the first and third quartiles). The whiskers show the minimum and maximum entry values.

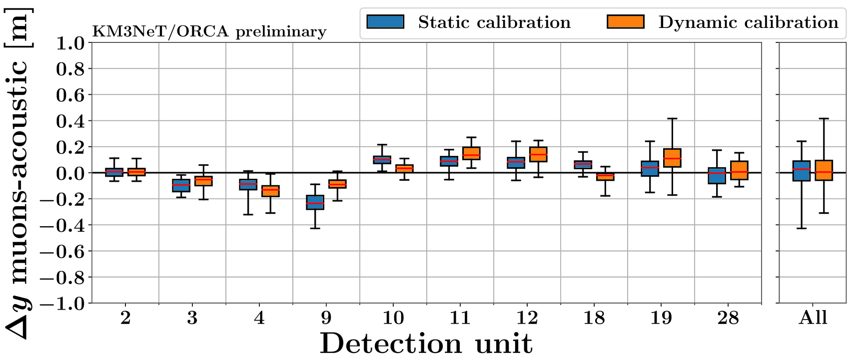

Figure 5: Distribution of the optimal y-position offset obtained with the track quality method with respect to the position calibration from acoustics, shown for each individual DU of ORCA and for all DUs. One entry is an optimal offset on a set of 5000 consecutive events. See Figure 4 for the definition of boxes and whiskers.

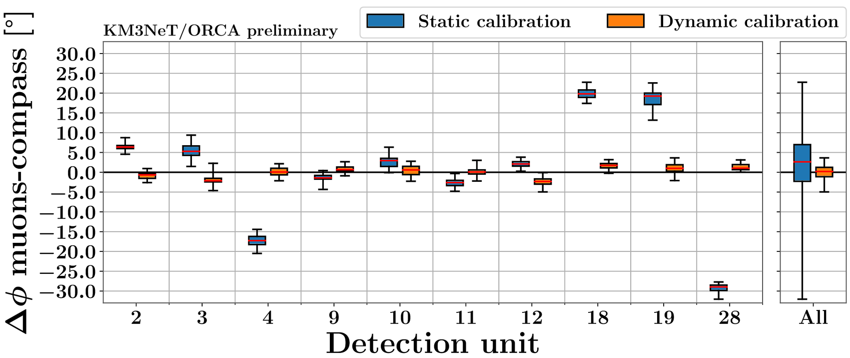

Figure 6: Distribution of the optimal orientation offset obtained with the track quality method with respect to the orientation calibration from compasses, shown for each individual DU of ORCA and for all DUs. One entry is an optimal offset on a set of 5000 consecutive events. See Figure 4 for the definition of boxes and whiskers.

4.2 Orientation calibration

For the ORCA detector, the muon track quality method agrees with the dynamic orientation calibration within a few degrees, as depicted in Figure 6, obtained with the same period used in Figure 5. This validates the calibration obtained with the compasses. Similar results are obtained with ARCA.

4.3 Time calibration

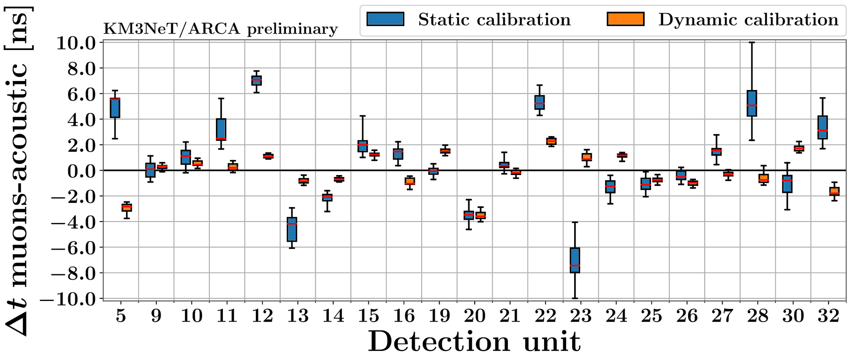

Figure 7: Distribution of the optimal time offset obtained with the track quality method with respect to the pre-existing calibration, for ARCA. One entry is an optimal offset on a set of 5000 consecutive events. See Figure 4 for the definition of boxes and whiskers.

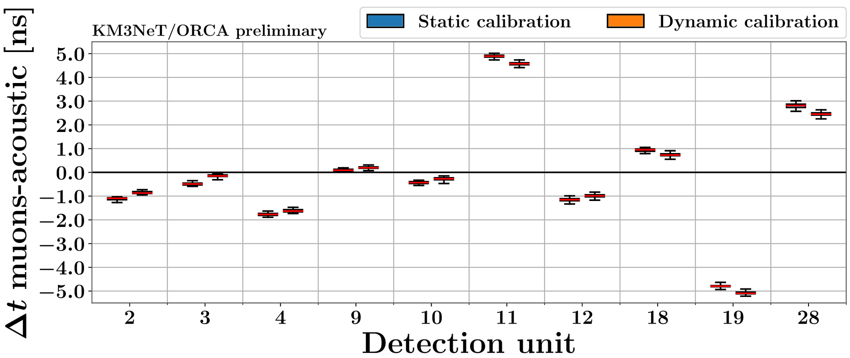

Figure 8: Distribution of the optimal time offset obtained with the track quality method with respect to the pre-existing calibration, for ORCA. One entry is an optimal offset on a set of 5000 consecutive events. See Figure 4 for the definition of boxes and whiskers.

Even though the time calibration does not result from the acoustic calibration procedure, the time offset obtained with the track quality method is still dependent on the acoustic calibration due to the degeneracy between the displacement of the DUs and the light arrival time. This is why a spreading in the optimal time offset value is seen in Figure 7. It is more pronounced when using static calibration for the same reason as for the position (DU movements not accounted for).

The offsets are also non-zero for some DUs, even in the dynamic case. This comes from remaining miscalibrations in the reference time of some DUs. More specifically, DUs 4, 11, 18, 19, and 28 of ORCA, which are the ones with the higher time offsets, were newly deployed DUs for the configuration studied here. It is thus expected that addiditional corrections to their time calibration are needed. The corrections to apply are the mean values of the offsets displayed in Figures 7 and 8.

The spread of the values when using dynamic calibration (thus correcting for DU movements) gives an idea of the accuracy of the muon track quality method for determining inter-DU time offsets. If we take the inter-quartile difference as reference metric (height of the boxes in Figure 7 and 8), it is around 0.3 ns for ARCA and 0.1 ns for ORCA. These values are consistent with the resolution values obtained from simulations [10], and satisfy the sub-nanosecond precision requirement on the time calibration. The better accuracy for ORCA is expected from the smaller distance between optical modules leading to a more precise muon track reconstruction.

5. Conclusion

Reconstructed muon tracks are used in KM3NeT for the inter-DU time calibration, achieving the required sub-nanosecond precision. The track quality method also allows to cross-check position and orientation calibrations, confirming the accuracy of the dynamic positioning and orientation procedure.

References

[1] S. Adrián-Martínez et al. (KM3NeT Collaboration), Letter of intent for KM3NeT 2.0, *J. Phys. G*, 43 (2016) 084001.

[2] S. Aiello et al. (KM3NeT Collaboration), The KM3NeT multi-PMT optical module, *J. Inst.*, 17 (2022) 07038.

[3] G. Riccobene on behalf of the KM3NeT Collaboration, The Positioning system for KM3NeT, *EPJ Web Conf.*, 207 (2019) 07005.

[4] C. Gatius Oliver on behalf of the KM3NeT collaboration, Dynamical position and orientation calibration of the KM3NeT telescope, in *PoSICRC2023* (2023) 1033.

[5] R. Coniglione on behalf of the KM3NeT collaboration, KM3NeT Time Calibration, in *PoSICRC2019* (2019) 868.

[6] S. Aiello et al. (KM3NeT Collaboration), Nanobeacon: A time calibration device for the KM3NeT neutrino telescope, *Nucl. Instrum. Methods Phys. Res. A*, 1040 (2022) 167132.

[7] A. Sánchez Losa on behalf of the KM3NeT collaboration, KM3NeT Time calibration with Nanobeacons, in *PoSICRC2023* (2023) 1062.

[8] M. Ageron et al. (KM3NeT Collaboration), Dependence of atmospheric muon flux on seawater depth measured with the first KM3NeT detection units, *Eur. Phys. J. C*, 80 (2020) 99.

[9] S. Aiello et al. (KM3NeT Collaboration), First observation of the cosmic ray shadow of the Moon and the Sun with KM3NeT/ORCA, *Eur. Phys. J. C*, 83 (2023) 344.

[10] D. Guderian, *Development of Detector Calibration and Graph Neural Network-Based Selection and Reconstruction Algorithms for the Measurement of Oscillation Parameters with KM3NeT/ORCA*, Ph.D. thesis, Münster University (Germany) (2022).

Full Authors List: The KM3NeT Collaboration

S. Aiello[a], A. Albert[b,bd], S. Alves Garre[c], Z. Aly[d], A. Ambrosone[f,e], F. Ameli[g], M. Andre[h], E. Androutsou[i], M. Anguita[j], L. Aphecetche[k], M. Ardid[l], S. Ardid[l], H. Atmani[m], J. Aublin[n], L. Bailly-Salins[o], Z. Bardačová[q,p], B. Baret[n], A. Bariego-Quintana[c], S. Basegmez du Pree[r], Y. Becherini[n], M. Bendahman[m,n], F. Benfenati[t,s], M. Benhassi[u,e], D. M. Benoit[v], E. Berbee[r], V. Bertin[d], S. Biagi[w], M. Boettcher[x], D. Bonanno[w], J. Boumaaza[m], M. Bouta[y], M. Bouwhuis[r], C. Bozza[z,e], R. M. Bozza[f,e], H.Brânzaş[aa], F. Bretaudeau[k], R. Bruijn[ab,r], J. Brunner[d], R. Bruno[a], E. Buis[ac,r], R. Buompane[u,e], J. Busto[d], B. Caiffi[ad], D. Calvo[c], S. Campion[g,ae], A. Capone[g,ae], F. Carenini[t,s], V. Carretero[c], T. Cartraud[n], P. Castaldi[af,s], V. Cecchini[c], S. Celli[g,ae], L. Cerisy[d], M. Chabab[ag], M. Chadolias[ah], A. Chen[ai], S. Cherubini[aj,w], T. Chiarusi[s], M. Circella[ak], R. Cocimano[w], J. A. B. Coelho[n], A. Coleiro[n], R. Coniglione[w] P. Coyle[d], A. Creusot[n], A. Cruz[al], G. Cuttone[w], R. Dallier[k], Y. Darras[ah], A. De Benedittis[e], B. De Martino[d], V. Decoene[k], R. Del Burgo[e], U. M. Di Cerbo[e], L. S. Di Mauro[w], I. Di Palma[g,ae], A. F. Díaz[j], C. Diaz[j], D. Diego-Tortosa[w], C. Distefano[w], A. Domi[ah], C. Donzaud[n], D. Dornic[d], M. Dörr[am], E. Drakopoulou[i], D. Drouhin[b,bd], R. Dvornický[q], T. Eberl[ah], E. Eckerová[q,p], A. Eddymaoui[m], T. van Eeden[r], M. Eff[n], D. van Eijk[r], I. El Bojaddaini[y], S. El Hedri[n], A. Enzenhöfer[d], G. Ferrara[w], M. D. Filipović[an], F. Filippini[t,s], D. Franciotti[w], L. A. Fusco[z,e], J. Gabriel[ao], S. Gagliardini[g], T. Gal[ah], J. García Méndez[l], A. Garcia Soto[c], C. Gatius Oliver[r], N. Geißelbrecht[ah], H. Ghaddari[y], L. Gialanella[e,u], B. K. Gibson[v], E. Giorgio[w], I. Goos[n], D. Goupilliere[o], S. R. Gozzini[c], R. Gracia[ah], K. Graf[ah], C. Guidi[ap,ad], B. Guillon[o], M. Gutiérrez[aq], H. van Haren[ar], A. Heijboer[r], A. Hekalo[am], L. Hennig[ah], J. J. Hernández-Rey[c], F. Huang[d], W. Idrissi Ibnsalih[e], G. Illuminati[s], C. W. James[al], M. de Jong[as,r], P. de Jong[ab,r], B. J. Jung[r], P. Kalaczyński[at,be], O. Kalekin[ah], U. F. Katz[ah], N. R. Khan Chowdhury[c], A. Khatun[q], G. Kistauri[av,au], C. Kopper[ah], A. Kouchner[aw,n], V. Kulikovskiy[ad], R. Kvatadze[av], M. Labalme[o], R. Lahmann[ah], G. Larosa[w], C. Lastoria[d], A. Lazo[c], S. Le Stum[d], G. Lehaut[o], E. Leonora[a], N. Lessing[c], G. Levi[t,s], M. Lindsey Clark[n], F. Longhitano[a], J. Majumdar[r], L. Malerba[ad], F. Mamedov[p], J. Mańczak[c], A. Manfreda[e], M. Marconi[ap,ad], A. Margiotta[t,s], A. Marinelli[e,f], C. Markou[i], L. Martin[k], J. A. Martínez-Mora[l], F. Marzaioli[u,e], M. Mastrodicasa[ae,g], S. Mastroianni[e], S. Miccichè[w], G. Miele[f,e], P. Migliozzi[e], E. Migneco[w], M. L. Mitsou[e], C. M. Mollo[e], L. Morales-Gallegos[u,e], C. Morley-Wong[al], A. Moussa[y], I. Mozun Mateo[ay,ax], R. Muller[r], M. R. Musone[e,u], M. Musumeci[w], L. Nauta[r], S. Navas[aq], A. Nayerhoda[ak], C. A. Nicolau[g], B. Nkosi[ai], B. Ó Fearraigh[ab,r], V. Oliviero[f,e], A. Orlando[w], E. Oukacha[n], D. Paesani[w], J. Palacios González[c], G. Papalashvili[au], V. Parisi[ap,ad], E.J. Pastor Gomez[c], A. M. Păun[aa], G. E. Păvălaş[aa], S. Peña Martínez[n], M. Perrin-Terrin[d], J. Perronnel[o], V. Pestel[ay], R. Pestes[n], P. Piattelli[w], C. Poirè[z,e], V. Popa[aa], T. Pradier[b], S. Pulvirenti[w], G. Quéméner[o], C. Quiroz[l], U. Rahaman[c], N. Randazzo[a], R. Randriatoamanana[k], S. Razzaque[az], I. C. Rea[e], D. Real[c], S. Reck[ah], G. Riccobene[w], J. Robinson[x], A. Romanov[ap,ad], A. Šaina[c], F. Salesa Greus[c], D. F. E. Samtleben[as,r], A. Sánchez Losa[c,ak], S. Sanfilippo[w], M. Sanguineti[ap,ad], C. Santonastaso[ba,e], D. Santonocito[w], P. Sapienza[w], J. Schnabel[ah], J. Schumann[ah], H. M. Schutte[x], J. Seneca[r], N. Sennan[y], B. Setter[ah], I. Sgura[ak], R. Shanidze[au], Y. Shitov[p], F. Šimkovic[q], A. Simonelli[e], A. Sinopoulou[a], M.V. Smirnov[ah], B. Spisso[e], M. Spurio[t,s], D. Stavropoulos[i], I. Štekl[p], M. Taiuti[ap,ad], Y. Tayalati[m], H. Tedjditi[ad], H. Thiersen[x], I. Tosta e Melo[a,aj], B. Trocmé[n], V. Tsourapis[i], E. Tzamariudaki[i], A. Vacheret[o], V. Valsecchi[w], V. Van Elewyck[aw,n], G. Vannoye[d], G. Vasileiadis[bb], F. Vazquez de Sola[r], C. Verilhac[n], A. Veutro[g,ae], S. Viola[w], D. Vivolo[u,e], J. Wilms[bc], E. de Wolf[ab,r], H. Yepes-Ramirez[l], G. Zarpapis[i], S. Zavatarelli[ad], A. Zegarelli[g,ae], D. Zito[w], J. D. Zornoza[c], J. Zúñiga[c], and N. Zywucka[x].

[a]INFN, Sezione di Catania, Via Santa Sofia 64, Catania, 95123 Italy
[b]Université de Strasbourg, CNRS, IPHC UMR 7178, F-67000 Strasbourg, France
[c]IFIC - Instituto de Física Corpuscular (CSIC - Universitat de València), c/Catedrático José Beltrán, 2, 46980 Paterna, Valencia, Spain
[d]Aix Marseille Univ, CNRS/IN2P3, CPPM, Marseille, France
[e]INFN, Sezione di Napoli, Complesso Universitario di Monte S. Angelo, Via Cintia ed. G, Napoli, 80126 Italy
[f]Università di Napoli "Federico II", Dip. Scienze Fisiche "E. Pancini", Complesso Universitario di Monte S. Angelo, Via Cintia ed. G, Napoli, 80126 Italy
[g]INFN, Sezione di Roma, Piazzale Aldo Moro 2, Roma, 00185 Italy
[h]Universitat Politècnica de Catalunya, Laboratori d'Aplicacions Bioacústiques, Centre Tecnològic de Vilanova i la Geltrú, Avda. Rambla Exposició, s/n, Vilanova i la Geltrú, 08800 Spain
[i]NCSR Demokritos, Institute of Nuclear and Particle Physics, Ag. Paraskevi Attikis, Athens, 15310 Greece
[j]University of Granada, Dept. of Computer Architecture and Technology/CITIC, 18071 Granada, Spain
[k]Subatech, IMT Atlantique, IN2P3-CNRS, Université de Nantes, 4 rue Alfred Kastler - La Chantrerie, Nantes, BP 20722 44307 France
[l]Universitat Politècnica de València, Instituto de Investigación para la Gestión Integrada de las Zonas Costeras, C/ Paranimf, 1, Gandia, 46730 Spain
[m]University Mohammed V in Rabat, Faculty of Sciences, 4 av. Ibn Battouta, B.P. 1014, R.P. 10000 Rabat, Morocco
[n]Université Paris Cité, CNRS, Astroparticule et Cosmologie, F-75013 Paris, France
[o]LPC CAEN, Normandie Univ, ENSICAEN, UNICAEN, CNRS/IN2P3, 6 boulevard Maréchal Juin, Caen, 14050 France
[p]Czech Technical University in Prague, Institute of Experimental and Applied Physics, Husova 240/5, Prague, 110 00 Czech Republic
[q]Comenius University in Bratislava, Department of Nuclear Physics and Biophysics, Mlynska dolina F1, Bratislava, 842 48 Slovak Republic
[r]Nikhef, National Institute for Subatomic Physics, PO Box 41882, Amsterdam, 1009 DB Netherlands
[s]INFN, Sezione di Bologna, v.le C. Berti-Pichat, 6/2, Bologna, 40127 Italy
[t]Università di Bologna, Dipartimento di Fisica e Astronomia, v.le C. Berti-Pichat, 6/2, Bologna, 40127 Italy
[u]Università degli Studi della Campania "Luigi Vanvitelli", Dipartimento di Matematica e Fisica, viale Lincoln 5, Caserta, 81100 Italy
[v]E. A. Milne Centre for Astrophysics, University of Hull, Hull, HU6 7RX, United Kingdom

[w] INFN, Laboratori Nazionali del Sud, Via S. Sofia 62, Catania, 95123 Italy
[x] North-West University, Centre for Space Research, Private Bag X6001, Potchefstroom, 2520 South Africa
[y] University Mohammed I, Faculty of Sciences, BV Mohammed VI, B.P. 717, R.P. 60000 Oujda, Morocco
[z] Università di Salerno e INFN Gruppo Collegato di Salerno, Dipartimento di Fisica, Via Giovanni Paolo II 132, Fisciano, 84084 Italy
[aa] ISS, Atomistilor 409, Măgurele, RO-077125 Romania
[ab] University of Amsterdam, Institute of Physics/IHEF, PO Box 94216, Amsterdam, 1090 GE Netherlands
[ac] TNO, Technical Sciences, PO Box 155, Delft, 2600 AD Netherlands
[ad] INFN, Sezione di Genova, Via Dodecaneso 33, Genova, 16146 Italy
[ae] Università La Sapienza, Dipartimento di Fisica, Piazzale Aldo Moro 2, Roma, 00185 Italy
[af] Università di Bologna, Dipartimento di Ingegneria dell'Energia Elettrica e dell'Informazione "Guglielmo Marconi", Via dell'Università 50, Cesena, 47521 Italia
[ag] Cadi Ayyad University, Physics Department, Faculty of Science Semlalia, Av. My Abdellah, P.O.B. 2390, Marrakech, 40000 Morocco
[ah] Friedrich-Alexander-Universität Erlangen-Nürnberg (FAU), Erlangen Centre for Astroparticle Physics, Nikolaus-Fiebiger-Straße 2, 91058 Erlangen, Germany
[ai] University of the Witwatersrand, School of Physics, Private Bag 3, Johannesburg, Wits 2050 South Africa
[aj] Università di Catania, Dipartimento di Fisica e Astronomia "Ettore Majorana", Via Santa Sofia 64, Catania, 95123 Italy
[ak] INFN, Sezione di Bari, via Orabona, 4, Bari, 70125 Italy
[al] International Centre for Radio Astronomy Research, Curtin University, Bentley, WA 6102, Australia
[am] University Würzburg, Emil-Fischer-Straße 31, Würzburg, 97074 Germany
[an] Western Sydney University, School of Computing, Engineering and Mathematics, Locked Bag 1797, Penrith, NSW 2751 Australia
[ao] IN2P3, LPC, Campus des Cézeaux 24, avenue des Landais BP 80026, Aubière Cedex, 63171 France
[ap] Università di Genova, Via Dodecaneso 33, Genova, 16146 Italy
[aq] University of Granada, Dpto. de Física Teórica y del Cosmos & C.A.F.P.E., 18071 Granada, Spain
[ar] NIOZ (Royal Netherlands Institute for Sea Research), PO Box 59, Den Burg, Texel, 1790 AB, the Netherlands
[as] Leiden University, Leiden Institute of Physics, PO Box 9504, Leiden, 2300 RA Netherlands
[at] National Centre for Nuclear Research, 02-093 Warsaw, Poland
[au] Tbilisi State University, Department of Physics, 3, Chavchavadze Ave., Tbilisi, 0179 Georgia
[av] The University of Georgia, Institute of Physics, Kostava str. 77, Tbilisi, 0171 Georgia
[aw] Institut Universitaire de France, 1 rue Descartes, Paris, 75005 France
[ax] IN2P3, 3, Rue Michel-Ange, Paris 16, 75794 France
[ay] LPC, Campus des Cézeaux 24, avenue des Landais BP 80026, Aubière Cedex, 63171 France
[az] University of Johannesburg, Department Physics, PO Box 524, Auckland Park, 2006 South Africa
[ba] Università degli Studi della Campania "Luigi Vanvitelli", CAPACITY, Laboratorio CIRCE - Dip. Di Matematica e Fisica - Viale Carlo III di Borbone 153, San Nicola La Strada, 81020 Italy
[bb] Laboratoire Univers et Particules de Montpellier, Place Eugène Bataillon - CC 72, Montpellier Cédex 05, 34095 France
[bc] Friedrich-Alexander-Universität Erlangen-Nürnberg (FAU), Remeis Sternwarte, Sternwartstraße 7, 96049 Bamberg, Germany
[bd] Université de Haute Alsace, rue des Frères Lumière, 68093 Mulhouse Cedex, France
[be] AstroCeNT, Nicolaus Copernicus Astronomical Center, Polish Academy of Sciences, Rektorska 4, Warsaw, 00-614 Poland

Acknowledgements

The authors acknowledge the financial support of the funding agencies: Agence Nationale de la Recherche (contract ANR-15-CE31-0020), Centre National de la Recherche Scientifique (CNRS), Commission Européenne (FEDER fund and Marie Curie Program), LabEx UnivEarthS (ANR-10-LABX-0023 and ANR-18-IDEX-0001), Paris Île-de-France Region, France; Shota Rustaveli National Science Foundation of Georgia (SRNSFG, FR-22-13708), Georgia; The General Secretariat of Research and Innovation (GSRI), Greece Istituto Nazionale di Fisica Nucleare (INFN), Ministero dell'Università e della Ricerca (MIUR), PRIN 2017 program (Grant NAT-NET 2017W4HA7S) Italy; Ministry of Higher Education, Scientific Research and Innovation, Morocco, and the Arab Fund for Economic and Social Development, Kuwait; Nederlandse organisatie voor Wetenschappelijk Onderzoek (NWO), the Netherlands; The National Science Centre, Poland (2021/41/N/ST2/01177); The grant "AstroCeNT: Particle Astrophysics Science and Technology Centre", carried out within the International Research Agendas programme of the Foundation for Polish Science financed by the European Union under the European Regional Development Fund; National Authority for Scientific Research (ANCS), Romania; Grants PID2021-124591NB-C41, -C42, -C43 funded by MCIN/AEI/ 10.13039/501100011033 and, as appropriate, by "ERDF A way of making Europe", by the "European Union" or by the "European Union NextGenerationEU/PRTR", Programa de Planes Complementarios I+D+I (refs. ASFAE/2022/023, ASFAE/2022/014), Programa Prometeo (PROMETEO/2020/019) and GenT (refs. CIDEGENT/2018/034, /2019/043, /2020/049. /2021/23) of the Generalitat Valenciana, Junta de Andalucía (ref. SOMM17/6104/UGR, P18-FR-5057), EU: MSC program (ref. 101025085), Programa María Zambrano (Spanish Ministry of Universities, funded by the European Union, NextGenerationEU), Spain; The European Union's Horizon 2020 Research and Innovation Programme (ChETEC-INFRA - Project no. 101008324).